The Madagascar Bloom: A serendipitous study

M. A. Srokosz[1] and G. D. Quartly[1,2]

Received 6 July 2012; revised 1 November 2012; accepted 1 November 2012; published 16 January 2013.

[1] The late austral summer (February–April) phytoplankton bloom that occurs east of Madagascar exhibits significant interannual variability and at its largest extent covers ~1% of the world's ocean surface area. The bloom raises many intriguing questions about how it begins, is sustained, propagates to the east, exports carbon, and ends. It has been observed and studied using satellite ocean color observations, but the lack of in situ data makes it difficult to address these questions. Here we describe observations that were made serendipitously on a cruise in February 2005. These show clearly for the first time the simultaneous existence of a deep chlorophyll maximum at ~70–110 m depths (seen in SeaSoar fluorimeter data) and a surface chlorophyll signature [seen in Sea-viewing Wide Field-of-view Sensor (SeaWiFS) satellite ocean color data]. The observations also show the modulation of the biological signature at the surface by the eddy field but not of the deep chlorophyll maximum. *Trichodesmium* dominates the bloom nearer to Madagascar, while the diatom *Rhizosolenia clevei* (and its symbiont *Richelia intracellularis*) dominates further from the island. The surface bloom seen in the SeaWiFS data is confined to the shallow (~30 m) mixed layer. It is hypothesized that the interannual variability in bloom intensity may be due to variations in coastal upwelling and thus the supply of iron, which is a micronutrient that can limit diazotroph growth.

Citation: Srokosz, M. A., and G. D. Quartly (2013), The Madagascar Bloom: A serendipitous study, *J. Geophys. Res. Oceans*, *118*, 14–25, doi:10.1029/2012JC008339.

1. Introduction

[2] *Longhurst* [2001] was the first to describe the seasonal development of a major bloom east of Madagascar, using ocean color observations from space [from POLDER and Sea-viewing Wide Field-of-view Sensor (SeaWiFS)]. He noted that the bloom typically occurred during the period February to April but was not present every year. The data showed that blooms had occurred in 1997, 1999, and 2000. Lacking in situ observations, *Longhurst* [2001] conjectured that the bloom was caused by the mixed layer deepening, a so-called entrainment bloom, but modulated by the presence of the eddy field. He speculated that the bloom might consist of nitrogen-fixing diazotrophic cyanobacteria *Trichodesmium* but considered it more likely to be due to larger eukaryotic algal cells (entrainment hypothesis).

[3] *Srokosz et al*. [2004] re-examined the bloom, also using ocean color data [Ocean Color and Temperature Scanner (OCTS) and SeaWiFS data for September 1996 to March 2004], and found an additional bloom in 2002. They advanced an explanation for the rapid spread of the bloom to the east away from Madagascar based on the interplay of plankton growth and diffusion (due to the eddy field), leading to the propagation of a possible "plankton wave." Their study was limited to examining the mechanism for bloom propagation.

[4] *Uz* [2007] studied the bloom using a combination of ocean color (SeaWiFS and Moderate Resolution Imaging Spectroradiometer), sea surface temperature [SST from Advanced Very High Resolution Radiometer (AVHRR)], in situ (Argo) and meteorological (re-analysis winds and wind stress curl, plus cyclone tracks) data. He discounted *Longhurst*'s [2001] entrainment hypothesis and advanced a new hypothesis based on iron limitation. He conjectured that tropical cyclones causing heavy rain on Madagascar wash iron-rich sediments into the coastal waters. These are then spread eastward by eddy diffusion and trigger a nitrogen-fixing diazotroph bloom when shallow mixed layers form due to heating of the upper ocean. The interannual variability in the cyclone tracks—whether or not they make landfall in Madagascar—is taken to explain the interannual variability of the bloom. Two criticisms can be made of this hypothesis: first, *Uz* [2007] invokes the eddy diffusion mechanism discussed by *Srokosz et al*. [2004] to explain the spread of iron eastwards. This misses the key point of that paper; namely, that it is the combination of plankton growth and eddy diffusion that allows the rapid eastward propagation of the bloom. For iron, there is no growth term and eddy diffusion is insufficient, on its own, to transfer material eastward sufficiently fast to explain the bloom propagation. Second, the main rivers on Madagascar drain to the west into the Mozambique Channel (as can be ascertained from an atlas) and thus do not contribute to the waters within the East Madagascar Current. Furthermore, the heavy rains associated with tropical cyclones occur mainly in northwest Madagascar and would

[1]National Oceanography Centre, Southampton, UK.
[2]Plymouth Marine Laboratory, Plymouth, UK.

Corresponding author: M. A. Srokosz, National Oceanography Centre, Southampton, SO14 3ZH, UK. (mas@noc.ac.uk)

2169-9275/13/2012JC008339

affect rivers flowing into the Mozambique Channel [*Nassor and Jury*, 1997, 1998].

[5] In contrast to *Uz* [2007], *Lévy et al*. [2007] concluded that the bloom is due to upwelling at the coast followed by transport to the east by the retroflection of the East Madagascar Current (EMC; on the possible retroflection of the EMC, see *Quartly et al*. [2006]; *Siedler et al*. [2009]). *Lévy et al*. [2007] and *Koné et al*. [2009] consider the evolution of the bloom only briefly, as part of a broader study of blooms in the Indian Ocean using SeaWiFS data and coupled ocean physics and ecosystem model output. Neither study reproduces the Madagascar bloom, primarily due to limitations of their biological models, although the spatial resolutions of the models may also be inadequate, given the bloom is dominated by mesoscale and sub-mesoscale features, which the models do not resolve.

[6] *Wilson and Qiu* [2008] have included the Madagascar bloom in their study of the global distribution of summer chlorophyll blooms in oligotrophic gyres (defined by *Wilson et al*. [2008] as chlorophyll >0.15 mg m^{-3}). They note that this is the only such bloom that exhibits eastward propagation (with the single exception of the 1997 bloom in the NE Pacific noted by *Wilson* [2003]). They suggest that the bloom is influenced by "island mass effects" developing within the dynamic eddy field and current system emanating off the southern tip of Madagascar. In particular, they associate it with the existence of the South Indian Ocean Counter Current (SICC; *Palastanga et al*. [2007]), which would allow consistent eastward migration. This is problematical as the link between the currents near Madagascar and the SICC remains to be established from in situ observations. The paper also suggests that the bloom occurs at the edges of regions of *Trichodesmium* occurrence and in an area of extremely low dust deposition (thus ruling out aeolian iron fertilization effects; as noted previously by *Srokosz et al*. [2004]). No explanation of the pronounced interannual variability of the Madagascar bloom is offered.

[7] The study by *Raj et al*. [2010] makes use of satellite, model, re-analysis, and hydrographic data and presents a large number of possible bloom mechanisms. Some of their explanations appear circular in that they use SeaWiFS data, output from a model that assimilates SeaWiFS data [*Gregg*, 2008], and estimates of *Trichodesmium* derived from SeaWiFS data [*Westberry and Siegel*, 2006] to support their view of the bloom. They conclude that *Trichodesmium* nitrogen fixers are involved in stimulating the bloom but, while mentioning the observations of *Poulton et al*. [2009], fail to note that these show that further to the east of Madagascar the dominant species is *Rhizosolenia clevei* (with symbiont *Richelia intracellularis*), while *Trichodesmium* are found mainly nearer to and to the south of Madagascar. They attribute the interannual variability of the bloom to a combination of upwelling, precipitation, light limitation, and mesoscale eddies.

[8] Most recently, *Huhn et al*. [2012] have applied Finite-Time Lyapunov Exponent and Finite-Time Zonal Drift analysis to altimetry-derived velocity fields south and east of Madagascar. Their results indicate the existence of eastward propagating jets, with the main jet at ~25°S forming a meridional transport boundary so limiting the spread of the bloom northwards. 25°S is a region of enhanced sea surface height variability, with eddy and/or Rossby wave propagation westward [*Quartly et al*., 2006]. The jet at 25°S can potentially transport iron from south of Madagascar so fertilizing the bloom. The jet exists in non-bloom years, and its interannual variability does not match that of the bloom, so this does not explain the latter behavior. *Huhn et al*. [2012] note that the plankton front propagates faster than the transport velocity of the jet.

[9] Therefore, many outstanding questions regarding the East Madagascar bloom remain unanswered: What are the causes of its significant interannual variability? What processes allow the bloom to occur in the oligotrophic gyre?; and By what mechanisms is it initiated and terminated? Several hypotheses exist in the literature, as noted above, but there are few data available to test them.

[10] This paper will not answer all the questions as the observations described below were obtained serendipitously! Rather, here the first combined physical, chemical, and biological in situ observations of the bloom are reported (an earlier paper *Poulton et al*. [2009] focused on biological measurements from the same cruise). These serendipitous observations allow us to draw some conclusions and answer some questions about the bloom, specifically the following:

- What, if any, is the link between the surface bloom observed in ocean color data and the subsurface physics and biology, and how does this relate to the eddy structures?
- How deep does the surface bloom penetrate into the water column?
- How do the subsurface measurements relate to the surface ones of *Poulton et al*. [2009]?

2. MadEx Cruise

[11] From 26 January to 21 February 2005, a cruise (called MadEx) took place on the RRS *Discovery* that was aimed at studying the East Madagascar Current and its interaction with the eddies to the south of Madagascar (see Figure 2b below for cruise region). Details of the cruise, its objectives, and the measurements made can be found in *Quartly* [2006]. The work included the deployment of moorings, measurements made using SeaSoar, conductivity-temperature-depth (CTD) casts, and underway biological and chemical sampling from the ship's non-toxic underway seawater supply (inlet depth at 5 m; see section 4). During the cruise, due to a medical emergency, it was necessary to divert RRS *Discovery* to the island of Réunion. This "lost" 5 days from the cruise program: 11 to 15 February. However, from satellite data, in particular ocean color observations (see Figure 1 and section 3 below) that were being received onboard, it was noted that a bloom to the east of Madagascar was present. Therefore, on the return journey from Réunion, SeaSoar was deployed on 14 February to make measurements concurrent with the underway sampling, thus giving the first (to our knowledge) in situ biological and physical data on the bloom. The need to prepare SeaSoar instruments for deployment meant that underway sampling from the ship's non-toxic underway seawater supply began earlier on the return journey than the SeaSoar measurements. Due to the lost time, there was an urgent need to return to the work area south of Madagascar and complete the planned cruise program. This meant that it was not possible to stop and sample the bloom in more detail. However, it did prove

possible, without too much loss of time, to execute slight course changes to allow the ship to pass through two eddies—one cyclonic and one anticyclonic (see Figure 1)—as eddies are known to play a key role in the development of the bloom [*Longhurst*, 2001]. The SeaSoar data described below cover the period 09.00 on 14 February to 05.44 on 16 February, ~45 h. As noted above, the underway biological and chemical sampling started closer to Réunion and provided data hourly for macronutrients (nitrate, phosphate, silicate) and chlorophyll *a* during this period. Underway sampling for phytoplankton species was more irregular.

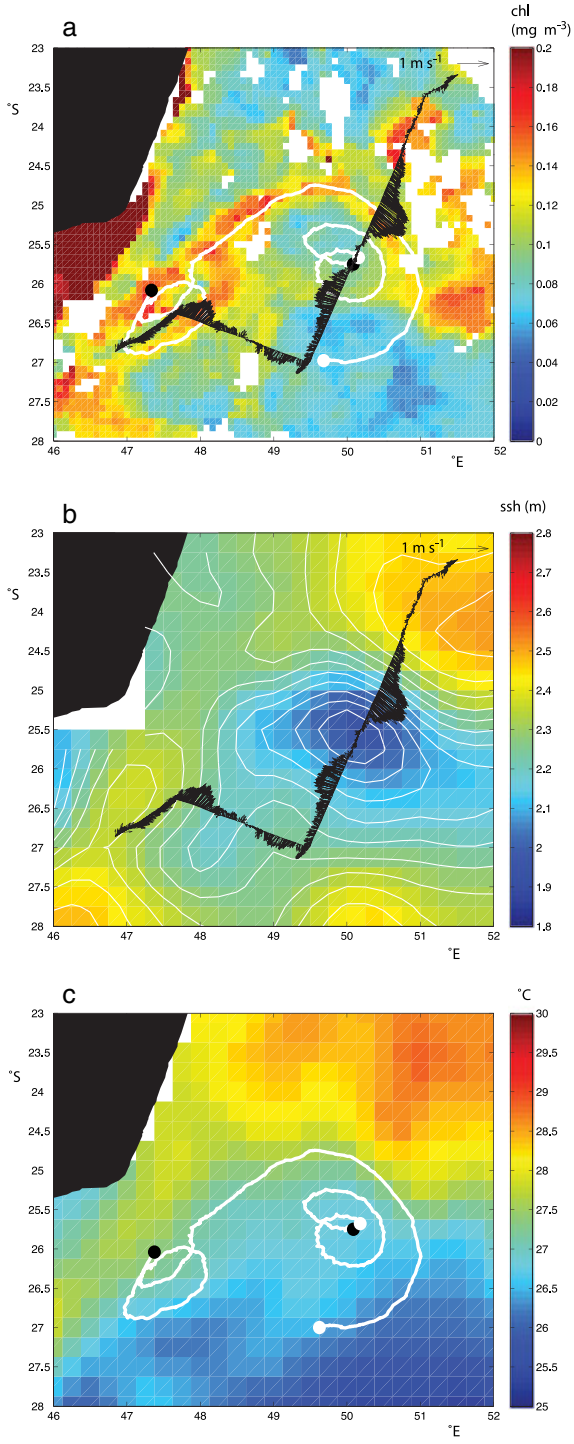

[12] Initial results for the phytoplankton species found in the surface waters, for the whole cruise, were published by *Poulton et al*. [2009]. They found that that the area to the south of Madagascar was dominated by *Trichodesmium*, while the bloom area to the east was dominated by *Trichodesmium* nearer to Madagascar but by diazotrophic diatoms (*Rhizosolenia clevei* with symbiont *Richelia intracellularis*) further to the east (see Figure 2 in *Poulton et al*. [2009]). This shows that nitrogen fixers play an important role in the southwest Indian Ocean. Here the context of those observations, just for the bloom area, is examined by using a combination of physical, chemical, and biological data from the cruise in conjunction with satellite ocean color data.

3. Satellite Observations

[13] Figure 1a shows an ocean color composite image from SeaWiFS covering the period 14 to 17 February. It was a similar image received onboard RRS *Discovery* that gave the first indication that that a bloom was present to the east of Madagascar. Overlaid on the image is that portion of the ship's track along which in situ observations were made using SeaSoar on the return from Réunion (see section 4 for the in situ observations). Figure 1b shows the corresponding altimetric absolute dynamic topography, and the high and low correspond to the eddies seen in the SeaWiFS data that the ship passed through. Figure 1c shows the SST in which the warm EMC flowing to the southwest can be clearly seen as it leaves the Madagascar coast, and this corresponds to the lower chlorophyll values in Figure 1a. The eddies that are evident in the SeaWiFS ocean color data and the absolute dynamic topography are difficult to discern in the SST (this was also the case when high-resolution Group for High Resolution Sea Surface Temperature data were examined—not

Figure 1. (a) Ocean color composite image for 14 to 17 February 2005. Four daily 9 km resolution SeaWiFS datasets are combined using the mean of their logarithms to avoid sensitivity to extreme high values. The track of the RRS *Discovery* is overlaid with its 75 kHz acoustic Doppler current profiler (ADCP) surface currents (in black), plus the trajectories of two satellite-tracked surface drifters (drogued at 15 m) deployed during the cruise. The track of the buoy deployed in the cyclonic eddy is for 20 days after deployment from the ship, while the track for the buoy in the anticyclonic eddy (deployed earlier in the cruise) is from 10 days prior to ship's passage to 20 days afterwards. Black dots mark the start of drifter tracks, white dots the end. The scale arrow represents a flow of 1 m s^{-1}. (b) Absolute dynamic height from altimetry, with height contours superimposed (every 5 cm), for the week centered on 16 February 2005. Data used are from AVISO's DUACS 0.25° "update" product, which uses all altimeter data available for that period. As in Figure 1a, the 75 kHz ADCP surface currents are overlaid (in black), with scale arrow representing a flow of 1 m s^{-1}. (c) Level 4 sea surface temperature (SST) interpolated product for 15 February 2005. Image shown is the 0.25° product from National Climatic Data Center, Asheville, NC, based on optimal interpolation of advanced very high resolution radiometer (AVHRR) data [*Reynolds et al.*, 2007]. Overlaid are the trajectories of two satellite-tracked surface drifters (details as for Figure 1a).

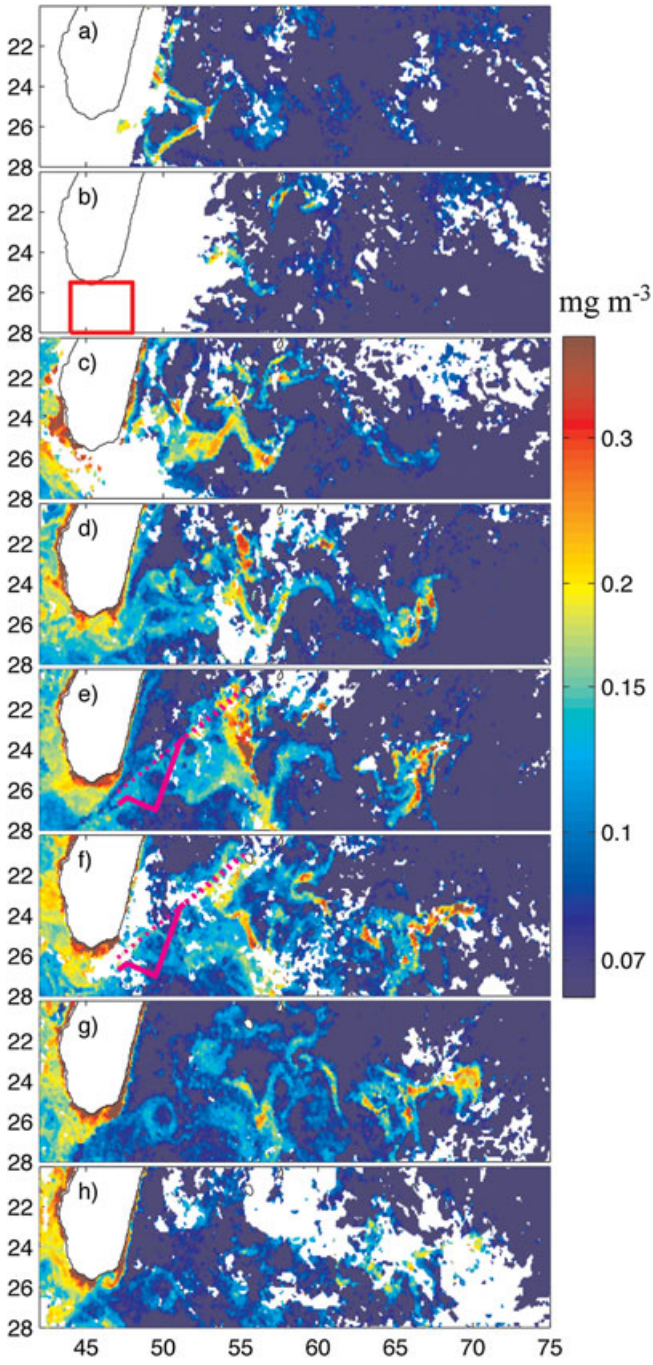

Figure 2. Sequence of SeaWiFS ocean color images (chlorophyll in mg m^{-3}) showing development of the bloom in 2005-7 day with a 3 × 3 median spatial filter applied: (a) 12–18 January; (b) 19–25 January; (c) 26 January to 1 February; (d) 2–8 February; (e) 9–15 February; (f) 16–22 February; (g) 23 February to 1 March; (h) 2–8 March. White areas are cloud covered. Red box in Figure 2b denotes the main MadEx study region. On Figures 2e and Figure 2f, the purple dotted line shows diversion to Réunion and the full purple line the track during SeaSoar deployment on return. The modulation of the bloom by the underlying mesoscale eddy field is clearly visible in the data. Note that the color scale differs from that in Figure 1a as the area shown is larger and the range of variability in chlorophyll is consequently greater.

shown). Enhanced surface chlorophyll levels occur around the periphery of both eddies, which is consistent with advection away from a source near Madagascar, but could also be due to submesoscale processes at the periphery of eddies [cf. *Calil and Richards* 2010].

[14] In Figure 2, the development and decline of the bloom is seen in a sequence of 7-day composites of SeaWiFS ocean color images, covering the period from 12–18 January to 2–8 March 2005. As noted by *Longhurst* [2001], the development of the bloom is clearly modulated by the mesoscale eddy field that exists to the east of Madagascar. The enhanced chlorophyll on the shelf around Madagascar, as well as the low chlorophyll of the EMC (just offshore to the east of the island), are both evident. Another striking feature in Figures 2d–2h is the cyclonic eddy that appears relatively stationary at around 50°E, 26°S. This is close to the location that was previously noted by *Quartly et al*. [2006] as a "parking place" for eddies, when their progression westward has halted for some (yet to be explained) reason. The in situ data were obtained during 14–16 February (see below), which overlaps the periods corresponding to Figures 2e and 2f, the later stages of the 2005 bloom. In Figure 2h, there is evidence of the spinning up of a cyclonic eddy inshore of the EMC, a phenomenon noted earlier by *Machu et al*. [2002].

[15] As stated in the introduction, the bloom has previously been observed in satellite ocean color data; here we observed a bloom in 2005 in the in situ data. However, it should be noted that there is some variation in how different authors assess the existence or absence of the bloom in specific years. While there is agreement on the years when a strong bloom exists, there is disagreement as to whether a bloom is weak or does not happen. *Uz* [2007] gives a numerical criterion for the existence/non-existence of the bloom; based the ratio of the mean chlorophyll over the bloom area (defined as 24–33°S, 48–66°E) to the mean chlorophyll over an area further east (defined as 24–33°S, 70–88°E; see his Figure 2b). He states that the bloom was absent in 2005, and only weak filaments were observed. This might seem at odds with the assessment here, but *Wilson and Qiu* [2008] describe the bloom in 2005 as "not as well-developed" but their criterion for a late summer bloom is that chlorophyll is greater than 0.15 mg/m^3, which differs from that of *Uz* [2007]. Therefore, at the time of the cruise (February 2005), it can be concluded that there was a bloom, but it did not develop as far, was not as strong, and did not persist for as long as those in strong bloom years (see the sequence of SeaWiFS images in Figure 10 of *Wilson and Qiu* [2008]).

[16] One final point to note from Figure 2 is that, while there is some evidence for the eastward propagation of the bloom in 2005, this appears to happen in two somewhat separated regions. One region nearer to Madagascar ~47–60°E (Figures 2a–2f) and another further away ~65–70°E (Figures 2d–2h). It is not clear that the development of the bloom follows an orderly progression from west to east.

4. In Situ Observations

[17] The data presented here from the MadEx cruise were obtained using underway sampling, acoustic Doppler current profiler (ADCP), and SeaSoar. The SeaSoar is a towed undulator and on this deployment carried standard CTD

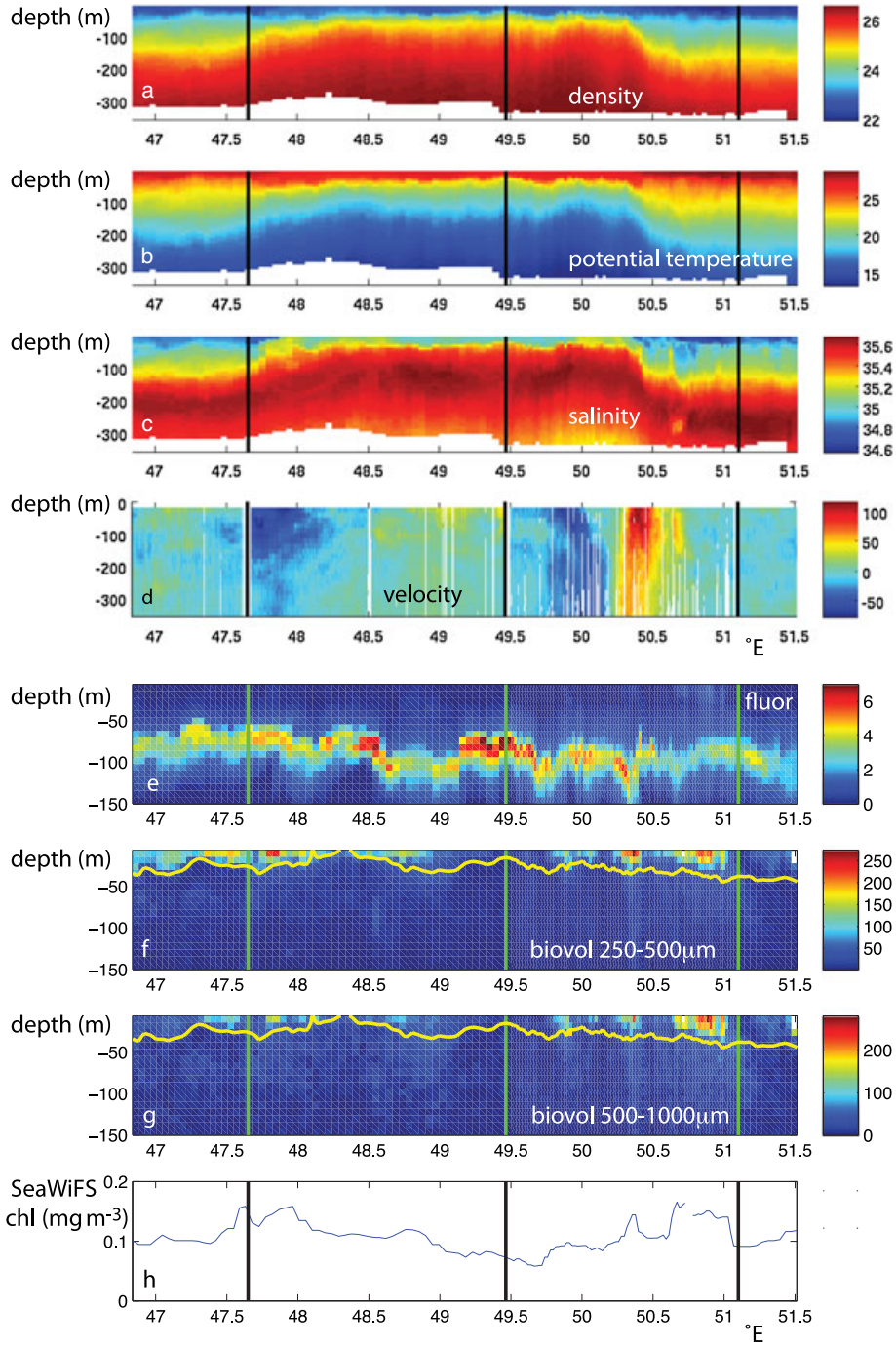

Figure 3. SeaSoar sections through bloom plotted against longitude. Top to bottom: (a) density (kg m^{-3}); (b) temperature (°C); (c) salinity; (d) cross-track currents from 75 kHz ADCP (positive to left of track as ship travels southwest, cm s^{-1}). Note that hull-mounted ADCP does not make measurements in the top few meters. (e) chlorophyll fluorescence (mg m^{-3}); (f) optical plankton counter (OPC) biovolume in size class 250–500 μm; (g) 500–1000 μm (mm^3 m^{-3}); (h) SeaWiFS surface chlorophyll (mg m^{-3}). The yellow contour in Figures 3f and 3g is that for potential temperature equal to 26.5°C. Note that chlorophyll fluorescence and OPC biovolume data are only shown for the top 150 m. Vertical lines mark where the ship changes course (see Figure 1).

sensors that measured temperature and salinity, a fluorimeter that measured chlorophyll fluorescence, and an optical plankton counter (OPC) that is designed to provide data on the abundance (no. m^{-3}) and biovolume (mm^3 m^{-3}) of mesozooplankton or particles in the size range 250–2000 μm. Here the data are analyzed in size classes 250–500, 500–1000, and 1000–2000 μm. We present data only for 250–500 and 500–1000 μm, as the measurements get noisier with

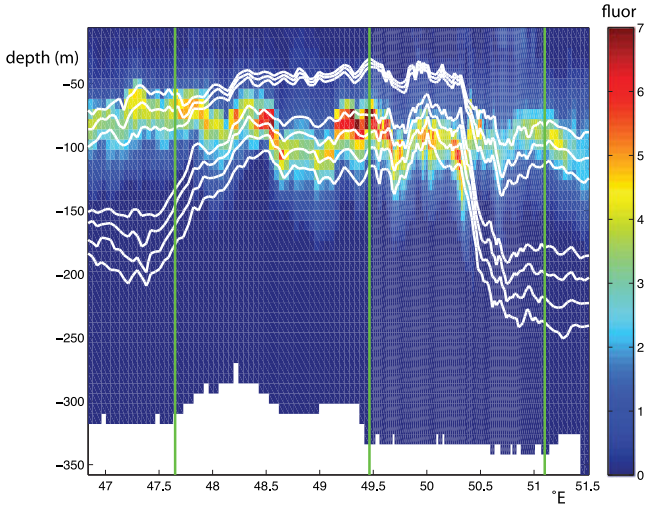

Figure 4. SeaSoar chlorophyll fluorescence data with density (kg m^{-3}) contours overlaid. Contours (shallowest to deepest) at 23.8, 24.0, 24.2, 25.0, 25.2, 25.4, and 25.6 kg m^{-3}. Vertical lines mark where the ship changes course (see Figure 1).

increasing size class due to the size of the OPC aperture (5 cm × 2 cm). SeaSoar was towed at 8 knots (~4 m s^{-1}) making measurements down to depths of ~300–350 m. The data were binned and averaged, and the results are presented on an 8 m by 5 km grid (5 km was chosen to ensure that one up and down traverse by SeaSoar is included in each bin). For more details of the instruments and processing, see *Quartly* [2006].

[18] Figure 3 shows the sections for density, temperature, salinity, chlorophyll fluorescence, and biovolume along the return track from Réunion. Note that the fluorescence calibration is that provided by the manufacturer, and no attempt has been made to calibrate it against in situ chlorophyll measurements due to the small amount of in situ data available (surface only and none at depth). Therefore, the fluorescence data are used simply as a qualitative indicator of chlorophyll. Clearly visible in the fluorescence (Figure 3e) is the deep chlorophyll maximum (DCM) at around 70–110 m (mean depth ~93 m). At this depth, the DCM will not be "seen" by satellite ocean color sensors due to the attenuation of the signal by the water column above [see *da Silva et al.* 2002; *Smith* 1981]. Therefore, the signatures visible in the satellite data (see Figure 1) must be due to very near surface phytoplankton chlorophyll that the SeaSoar fluorimeter does not detect very well due to the quenching effects of sunlight. Therefore, here we use the SeaWiFS surface chlorophyll observations rather than the SeaSoar ones. SeaWiFS surface chlorophyll data along the SeaSoar track are also shown in Figure 3h.

[19] To examine the DCM more closely and to see whether it has any relationship to the eddies that clearly modulate the surface chlorophyll (see Figure 1), the SeaSoar fluorescence with density contours overlaid is plotted in Figure 4. Along the transect, the DCM stays at a relatively constant depth, between ~70–110 m, whereas the isopyncals change depth by as much as ~150 m across the eddy features. There is also no clear relationship between the chlorophyll levels in the DCM and the background eddy field. Similar plots for fluorescence with temperature and salinity contours overlaid (not shown) also do not reveal any clear relationship with the mesoscale (eddy) structures. This is true for both the intensity and depth of the DCM.

[20] The OPC biovolume data in size classes 250–500 and 500–1000 μm (Figures 3f and 3g) suggest that the highest concentrations of particles are near the surface, in the top ~30 m, not at the DCM. This could be because the OPC cannot measure microzooplankton (<200 μm) that may be present in the vicinity of the DCM (it would "see" mesozooplankton >250 μm). By examining vertical profiles of density, temperature, and salinity (not shown), it was found that the mixed layer depth is ~30 m along the SeaSoar transect. This suggests that whatever is causing the signal in the OPC, mesozooplankton or something else (see discussion in section 5 below), is confined by summer stratification to the shallow mixed layer. The depth to which the increased biovolume and abundance are seen is roughly delimited by the 26.5°C temperature contour (see Figures 3f and 3g). Neither salinity nor density gave such a clear delimitation of the increased biovolume and abundance.

[21] The RRS *Discovery* has two hull-mounted ADCP instruments operating at 75 and 150 kHz, which allowed us to make underway measurements of the currents. Since the 75 kHz ADCP has greater depth penetration (~900 m), we show results from that instrument (with 16 m vertical and ~0.5 km along-track resolution; the latter corresponding to 2 min sampling; see *Quartly* [2006]). Those obtained from the 150 kHz ADCP are similar but only give data for the upper ~350 m of the water column. Figure 1a shows the surface currents, while Figure 3d shows the cross-track current component. These confirm the presence of the mesoscale eddies seen in the satellite data and show that the maximum velocities at the surface can reach ~1 ms^{-1}. The full-depth 75 kHz ADCP data (not shown) indicate that velocity structure penetrates down to at least 600 m for the cyclonic eddy [cf. *Donohue and Toole* 2003, Figure 10], while it seems to be confined more to the top 200 m for the anticyclonic one. In both cases, the velocity structure penetrates much deeper than the DCM observed in the SeaSoar data.

[22] During the cruise, a number of satellite-tracked surface drifters, drogued at 15 m, were deployed. The tracks of two, one deployed prior to the diversion to Réunion and one deployed on the return leg, are shown in Figure 1a confirming the presence of the cyclonic and anticyclonic eddies evident in the SeaWiFS chlorophyll images and ADCP currents.

[23] The cyclonic eddy centered ~(49.5°E, 25.5°S) is clearly discernible—doming up of isopycnals—in the density, temperature, and salinity observations at ~49.5–50.5°E, where the SeaSoar track intersects the eddy (Figure 3). A simple calculation, based on the ADCP data down to 600 m, shows a transport of 21.7 sverdrup (Sv) to the east in the northern half of the eddy and 17.7 Sv to the west in the southern half. Here, for the purpose of the calculation, the eddy is delimited 48.8–50.6°E in longitude, with center at 50.2°E; but defining the edge is problematical given that it is embedded in a complex flow field. Furthermore, the SeaSoar track does not pass through the actual center of

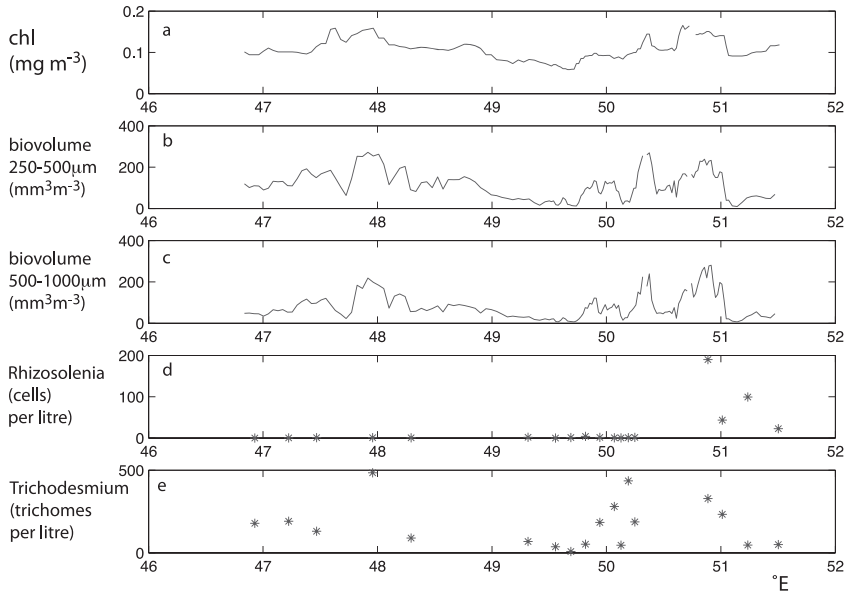

Figure 5. Surface values along SeaSoar transect (top to bottom): (a) SeaWiFS chlorophyll (mg m^{-3}), (b) OPC biovolume in size class 250–500 μm (mm^3 m^{-3}), (c) OPC biovolume in size class 500–1000 μm (mm^3 m^{-3}), (d) *Rhizosolenia* abundance (cells per liter), and (e) *Trichodesmium* abundance (trichomes per liter).

the eddy. Calculating the transport from 200–600 m gives 12.9 Sv to the east and 12.4 Sv to the west, a more balanced result. As can be seen from Figures 1 and 3d, the flow near the surface (approximately the top 200 m) is intensified to the east.

[24] The anticyclonic eddy, centered at ~(47.3°E, 26.7°S), is less discernible in the SeaSoar data as it is more elongated in a southwest direction (Figure 1). This is due to the underlying bathymetry and because satellite sea surface height data (not shown) suggest that it has recently separated from a larger anticyclonic feature to the north. The strong currents at one edge are clearly seen but are confined more to the top 200 m of the water column (Figure 3d). The doming up and down of isopycnals is suggestive of an intra-thermocline eddy (ITE) as found in the area previously by *Nauw et al*. [2006] but centered on a shallower depth ~100 m rather than ~200 m as found by *Nauw et al*. [2006]. However, the temperature and salinity properties differ from those of the ITEs observed by *Nauw et al*. [2006]—here at 100 m depth they are ~23° and ~35.2, as compared to ~20° and ~35.8 at 200 m [*Nauw et al*., 2006], so warmer and fresher.

[25] There is a subsurface salinity maximum of ~35.65 at depths of ~270 m at the northern end of the SeaSoar track, shallowing to ~130 m and the deepening again to ~200 m at the southwestern end (Figure 3c). In the cyclonic and anticyclonic eddies, the value of salinity at the maximum and the depth of the maximum are similar to those found for cyclonic and anticyclonic eddies in the Mozambique Basin by *de Ruijter et al*. [2004]. This indicates that such eddies can cross the Madagascar Ridge from the east of Madagascar into the Mozambique Basin (cf. Figure 9 of *de Ruijter et al*. [2004]).

[26] To further examine the link between the SeaWiFS surface observations and the SeaSoar ones, along-track surface chlorophyll values were taken from SeaWiFS data that were within 6.7 km of the locations of the gridded SeaSoar data (see Figure 5; given the resolution of the data, the choice of 6.7 km ensures that there will be at least one match-up within the search radius). While a comparison between the SeaWiFS and SeaSoar surface chlorophyll is not informative, due to surface quenching affecting the SeaSoar fluorimeter data, a surprising result was found when a comparison was made between SeaWiFS chlorophyll and biovolume from the OPC. Figures 5 and 6 show that the SeaWiFS chlorophyll is well correlated with the biovolume in the size classes 250–500 and 500–1000 μm (correlation coefficients of 0.78 and 0.76, respectively), which are also well correlated with each other (0.90). A similar result holds for OPC abundances (0.79, 0.78, 0.94). These correlations are reminiscent of similar ones found by *Srokosz et al*. [2003] during the North Atlantic spring bloom, where they were indicative of predator-prey dynamics—phytoplankton being grazed by zooplankton and both being eaten by larger zooplankton. Whether this is the explanation for what is observed here will be considered further in the discussion below.

[27] The biological and chemical sampling that was carried out on the cruise is fully described by *Poulton et al*. [2009] so will only briefly be considered here, with a specific focus on the samples taken along the SeaSoar transect. For biological and chemical analysis, water samples were collected from the ship's non-toxic underway seawater supply (inlet depth 5 m) every hour for measurements of chlorophyll *a* and macronutrients (nitrate, phosphate, silicate), and every 2–4 h for large (>50 μm) diazotrophs. Diazotroph abundance was measured on large volume (10 L) water samples, which were slowly concentrated down to ~20 mL by gentle removal of seawater through a 50 μm nylon mesh

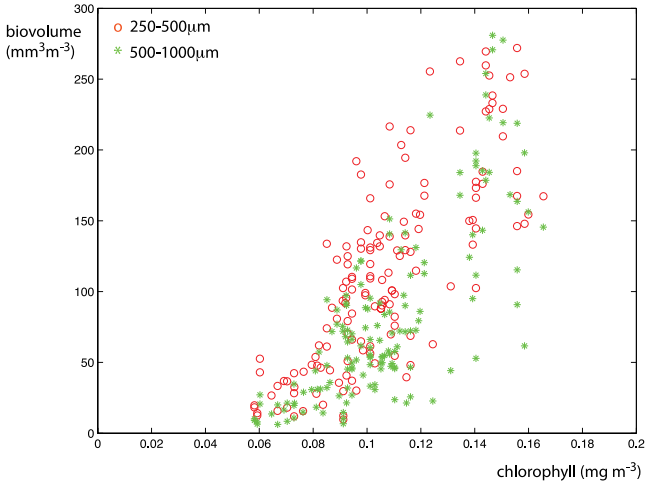

Figure 6. OPC biovolume in size classes 250–500 μm (red circles, mm^3 m^{-3}) and 500–1000 μm (green asterisks, mm^3 m^{-3}) plotted against SeaWiFS surface chlorophyll (mg m^{-3}).

and preserved with 2% acidic Lugol's solution in 25 mL glass vials. The abundance of *Trichodesmium* colonies, individual trichomes, and diatom cells (per liter) were determined in the full preserved volume using a 25 mL Bogorov tray and binocular microscope. Colonies of *Trichodesmium* were converted into trichome numbers assuming each colony consisted of 200 trichomes (for more details, see *Poulton et al*. [2009] and *Quartly* [2006]).

[28] Figure 5 shows the abundance of *Rhizosolenia* cells and *Trichodesmium* trichomes along the transect. While there is some relationship between the in situ abundances and both the SeaWiFS chlorophyll and OPC biovolume, there are insufficient numbers of in situ samples to draw strong conclusions. Nevertheless, the observations are suggestive that SeaWiFS is seeing the chlorophyll signature of *Rhizosolenia*, with its symbiont *Richelia*, and *Trichodesmium*. Taken in conjunction with the results of *Poulton et al*. [2009, Figure 2], there seems to be an indication that if *Trichodesmium* is present then *Rhizosolenia* is not, and vice-versa (although there is some overlap around 51°E on the transect; Figure 5).

[29] Figure 7 shows the SeaWiFS and in situ chlorophyll, together with nutrients (nitrate + nitrite, silicate, phosphate) at the surface along the SeaSoar track. The SeaWiFS and in situ chlorophyll show good agreement (mean difference, SeaWiFS minus in situ, of −0.01 mg m^{-3}). Nitrate + nitrite and phosphate values are low, while silicate ones are not. The low values of nitrate + nitrite are consistent with the presence of nitrogen fixers. *Poulton et al*. [2009] noted that, over the whole cruise, the main areas of *Rhizosolenia* abundance were associated with silicate concentrations <1 μmol kg^{-1}, but Figures 5 and 7 suggest this is not the case for the section of SeaSoar track studied here. Recollect that their paper presented results from the whole cruise, whereas here the focus is only on the SeaSoar observations of the bloom area, and the high abundances of *Rhizosolenia* found by *Poulton et al*. [2009] lie beyond the end of the SeaSoar track further northeast towards Réunion.

[30] There is a weak negative correlation (−0.50; data not shown) between the SeaWiFS surface chlorophyll and the fluorescence at the DCM. Increased chlorophyll concentration at the surface and the associated higher abundance of *Trichodesmium* or *Rhizosolenia* could both lead to less light penetration to depth and so stronger light limitation and less chlorophyll at the DCM. As the surface values of chlorophyll are low, it is unlikely that the chlorophyll on its own will affect the light levels at depth significantly, but the presence of higher abundances of *Trichodesmium* or *Rhizosolenia* almost certainly will. In similar circumstances, *Villareal et al*. [2011] found a significant impact of diatoms on their

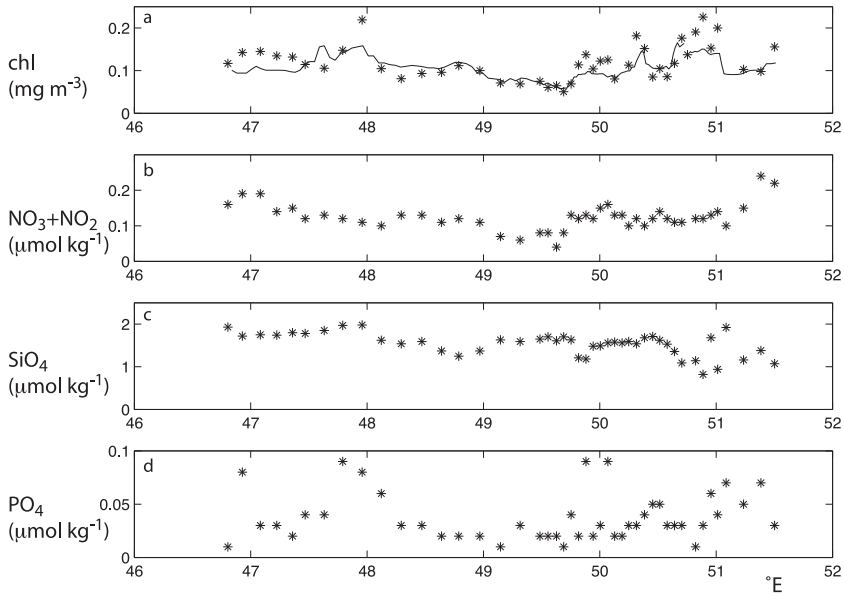

Figure 7. Surface values along SeaSoar transect (top to bottom): (a) SeaWiFS chlorophyll (mg m^{-3}) with in situ chlorophyll (asterisk; mg m^{-3}), (b) nitrate + nitrite (μmol kg^{-1}), (c) silicate (μmol kg^{-1}), and (d) phosphate (μmol kg^{-1}).

transmissometer measurements (a point that will recur in the discussion below).

5. Discussion

[31] Having described the observations made during the cruise, we now turn to a consideration of the possible explanations for what was observed.

5.1. DCM

[32] We have made the first observations of a DCM contemporaneous with a surface Madagascar bloom. The depth of the DCM does vary along the SeaSoar transect (Figure 4) and is probably set by the availability of light and the depth of the nitracline (recalling from Figure 7 that the surface waters are depleted of nitrate). Unfortunately, there are no subsurface nutrient measurements with which to verify this. With regard to light levels, a simple calculation (following *da Silva et al*. [2002]), assuming a diffuse attenuation for light of 0.05 m^{-1}, gives a euphotic (1% of surface light) depth of 92 m, which is about the same value as the mean depth of the DCM. The depth of the nitracline might be weakly modulated by the presence of eddies (as found by *Pidcock et al*. [2010]); thus, mesoscale structures might influence the DCM indirectly, but such an effect is not clearly seen in Figure 4. The DCM is not visible in the OPC data, which suggests that it is dominated by different phytoplankton species to those forming the surface bloom. However, not having in situ water samples for the DCM means that it is not possible to be definitive on this point. Output from a global ecosystem model available at the National Oceanography Centre [*Yool et al*., 2011] for the location and time of year of the cruise reveals the existence of a DCM but no surface bloom. In the model, the DCM exists for most of the year but seems to be disrupted by deeper mixing during the austral winter (July to September). The lack of a surface bloom in the model is unsurprising, as the ecosystem model does not include the nitrogen fixers that were observed on MadEx in the surface waters. The DCM SeaSoar observations and model results are consistent with what might be expected in the late summer for an ecosystem in an oligotrophic subtropical gyre formed due to the phytoplankton's requirement for both nutrients and light.

5.2. Surface Bloom

[33] It is unlikely that the OPC (see Figures 3, 5, and 6) is measuring the presence of mesozooplankton, as was the case in *Srokosz et al*.'s [2003] observations. As no zooplankton net sampling was possible, this cannot be proved conclusively. However, the size class 250–500 μm abundance (no. L^{-1}; units chosen for ease of comparison with *Poulton et al*. [2009]) is in the range 0–12, while for the size class 500–1000 μm it is in the range 0–3. *Poulton et al*. [2009] suggest that each *Trichodesmium* colony contains about 200 trichomes. So from the in situ data in Figure 5, we estimate 0–2.5 *Trichodesmium* colonies per liter along with 0–200 diatom cells per liter. *Poulton et al*. [2009] also note that diatom dimensions were 200–800 μm by 40–60 μm (mean value 474 μm by 47 μm), so potentially detectable by the OPC. Given that *Trichodesmium* colonies can be of significant size O(cm) and that *Rhizosolenia* can also form assemblages or associations O(cm) [cf. *Villareal et al*. 2011 and references therein], the in situ and OPC estimates of abundance are not dissimilar. Therefore, most likely the OPC is giving some measure of the abundance of *Trichodesmium* and *Rhizosolenia* in the shallow mixed layer. As the high values of both OPC biovolume and abundance are delimited in depth by the 26.5°C isotherm, this is consistent with optimal growth conditions for *Trichodesmium* and *Rhizosolenia*, as noted by *Wilson and Qiu* [2008] and *Breitbarth et al*. [2007]. These observations show similarity to those of *Villareal et al*. [2011]. In studying summer blooms of diatom-diazotroph assemblages (DDAs) in the North Pacific gyre, they found that these could be seen clearly in transmissometer (optical) data but did not have strong chlorophyll signatures. They defined a DDA bloom as abundances $>10^5$ cells m^{-3}. Here, in the chlorophyll filaments (Figure 1 and 5), we have *Rhizosolenia* abundances of up to 200 cells L^{-1} that is 2×10^5 cells m^{-3}, which meets their criterion, with even larger values further east (see Figure 2d of *Poulton et al*. [2009]). However, some optical methods for counting colonies or DDAs could be sensitive to the effects of turbulent flow, such as that which might be encountered at the OPC aperture as it is towed through the water or in a pumped underway water sampling system. The turbulence could cause the colonies or DDAs to break up, leading to uncertainty in the estimates of numbers and size. One way to determine the actual number of colonies or assemblages would be to use an instrument like the video plankton recorder, as was done in the Atlantic by *Davis and McGillicuddy* [2006].

[34] The observation that *Trichodesmium* are more abundant closer to Madagascar supports *Westberry and Siegel*'s, [2006, Figure 3a and 3d] SeaWiFS (1998–2003) based estimates of how often such blooms occur globally. Their estimates do not indicate the presence of *Trichodesmium* further to the east but mainly to the south of and closer to but east of Madagascar, consistent with *Poulton et al*.'s [2009] in situ observations. *Poulton et al*. [2009] give estimates of the nitrogen fixation rates for the Madagascar bloom and show that these are significant ($<$0.5 mmol N m^{-2} day^{-1} for *Trichodesmium*, 0.4–2.4 mmol N m^{-2} day^{-1} for diazoptrophic diatoms in the bloom region, comparable with estimates for other ocean regions). The observations also cohere with the modeling of nitrogen fixers by *Monteiro et al*. [2010, 2011], which show pronounced variability over a year in *Trichodesmium* and DDA analogs to the east of Madagascar [*Monteiro et al*., 2010 Figure 3b and 3d], with the DDA analogs showing great variability. Unfortunately, they do not indicate when during the year that variability occurs so it may or may not be at the time of the observed Madagascar bloom. *Monteiro et al*. [2011, Figure 4 as compared to Figure 1a] show that the total diazotroph biomass is increased east of Madagascar when they increase iron solubility in their model. This suggests that iron might play a key role in the actual bloom. Note, however, that the *Monteiro et al*. [2010, 2011] global model is of $1° \times 1°$ spatial resolution so does not capture the effects of the eddy field.

5.3. Causes of the Bloom

[35] If the dominant species are nitrogen fixers, could the Madagascar bloom be being stimulated by the input of iron (potentially a limiting micronutrient) as suggested by *Uz* [2007]? A recent review of aeolian iron deposition [*Mahowald et al*., 2009] would suggest that this is too small in the

Madagascar bloom region to significantly impact phytoplankton growth through iron fertilization ($<$0.01 g Fe m^{-2} yr^{-1}, as compared to Saharan dust deposition in the Atlantic $>$0.2 g Fe m^{-2} yr^{-1} which is known to have a fertilizing effect [*Marañón et al*., 2010]). A more likely source of iron are the sediments in the shallower waters on the continental shelf south of Madagascar which, if advected east, could cause the bloom in a similar way that the blooms around Kerguelen [*Blain et al*., 2007] and Crozet [*Pollard et al*., 2009] are formed. However, the strong interannual intermittency of the bloom suggests that any release of iron from the sediments and into the surface waters must also be strongly variable interannually (the Crozet bloom exhibits significant interannual variability too; *Pollard et al*. [2007]). To the authors' knowledge, no data exist on the release of iron from the sediments around Madagascar. Any release of iron from the sediments into the surface waters could be related to the upwelling that occurs to the south of Madagascar, which is thought to be variable interannually [*DiMarco et al*., 2000; *Lutjeharms and Machu*, 2000; *Machu et al*., 2002]. *DiMarco et al*. [2000] note that the upwelling depends on both the wind field and the behavior of the EMC, while *Lutjeharms and Machu* [2000] and *Machu et al*. [2002] show that that cyclonic eddy inshore of the EMC also affects the upwelling. As the upwelling variability is affected by the winds, the EMC, and the eddy at the southern tip of Madagascar—none of which are sufficiently well understood individually nor well characterized by existing observations—their combined effects are even less certain. The transport of the iron to the east would be also be determined by the behavior of the eddy field and SICC [*Srokosz et al*., 2004; *Palastanga et al*., 2007; *Huhn et al*., 2012].

5.4. Eddies and the SICC

[36] For the cyclonic eddy, there is a near-surface (top 200 m) intensification of the transport to the east relative to the west of about 4 Sv. This occurs at about 25°S, the latitude of the SICC [*Palastanga et al*., 2007; *Huhn et al*., 2012]. *Nauw et al*. [2008] estimate an SICC transport of 3 to 6 Sv, while *Huhn et al*.'s [2012] SICC propagation speed of 0.14 m s^{-1} can be transformed into a transport estimate of 2.1 to 5.25 Sv by assuming that the SICC has a width of 100 to 150 km over a depth of 150 to 250 m (based on *Palastanga et al*. [2007] Figure 5). Assuming the strengthening of the westward flow in the upper 200 m of the eddy is caused by the presence of the SICC, the degree of intensification is consistent with these other estimates of SICC transport. However, this is an instantaneous transport estimate, and the agreement with previous observations may be fortuitous given the intermittent nature of the SICC flow in a turbulent eddy field.

5.5. What Limits the Propagation of the Bloom?

[37] Here the results of *Mognin et al*. [2009] for the Kerguelen bloom are suggestive. Essentially, the summer bloom depletes the iron advected from Kerguelen in the winter, at which point the bloom ceases. A similar scenario can be envisaged for the Madagascar bloom. Iron is upwelled from sediment near Madagascar and transported eastwards causing a bloom that lasts until the iron is exhausted. Interannual variability in the size of the bloom is caused by interannual variability in the strength of the upwelling. Note that the advection of the iron would occur prior to the formation of the bloom, and it would then be some other factor that gives the bloom its apparent eastward propagating behavior. Such an iron advection effect would be consistent with the results of *Srokosz et al*. [2004] and *Huhn et al*. [2012]. The presence of advected iron together with the shallowing of the mixed layer during the summer could lead to a bloom, as warm, stably stratified waters allow nitrogen fixers to flourish [*Capone et al*., 1997; *Wilson and Qiu*, 2008]. In 2005 (Figure 2), it is not clear that the bloom propagates eastward, as it occurs earlier at ~65°E than at ~60°E. Thus, the bloom may develop by some combination of mixed layer shallowing and a mechanism that allows eastward propagation.

5.6. A Possible Scenario

[38] Pulling together the results of this and previous studies, a potential scenario for the late summer Madagascar bloom emerges. The bloom is constituted of *Trichodesmium* and diatom-diazotroph assemblages, although not necessarily in coexistence. It may be fertilized by iron carried eastwards from the upwelling region south of Madagascar, with consumption of the iron ultimately limiting the spread of the bloom. It could be triggered by the warming and shallowing of the mixed layer in the summer, allowing nitrogen fixers to bloom. The interannual variability in the strength of the bloom would then be determined by variations in the strength of the upwelling from year to year. An outstanding challenge is to characterize the variability of the upwelling and see if it displays any relationship to the interannual intermittency of the bloom. A further challenge would be to determine whether iron flux from the sediments could support the bloom.

6. Conclusions

[39] The exact mechanisms for the formation, propagation, and extinction of the Madagascar bloom are still unclear, but the in situ observations from the MadEx cruise presented here and by *Poulton et al*. [2009] have clarified some aspects of the bloom. The only way to determine the behavior of the complex biological, chemical, and physical processes affecting the Madagascar bloom would appear to be to mount a multi-year in situ observational program that would capture both stronger and weaker bloom events and the beginning and end of the bloom. It would also need to have a fuller biological, chemical, and physical sampling program than was possible on the cruise in 2005. For example, measurements of iron (in water and potential aeolian deposition), water samples for phytoplankton species composition at the surface and at the DCM, vertical zooplankton net hauls (also for species composition), and direct determination of export flux are among the extra information that is required.

[40] However, the data that were obtained serendipitously on the MadEx cruise allow the following new insights into the bloom:

- A deep chlorophyll maximum (mean depth ~93 m) and a surface chlorophyll bloom are found to exist simultaneously.
- The surface biological signature is modulated by the eddy field, but the deep chlorophyll maximum does not seem to be.

- The surface bloom seen in ocean color data is confined to the shallow (~30 m) mixed layer.
- Nitrogen fixers play a key role in the Madagascar blooms visible in satellite ocean color data. *Trichodesmium* dominates near to Madagascar, while *Rhizosolenia/Richelia* dominates further to the east, and both are detected by the OPC due to their organization into colonies and assemblages.
- The surface bloom and the DCM are likely composed of different phytoplankton species, as the OPC detects the former but not the latter.

[41] These observations further our understanding of the bloom, but, in agreement with *Uz* [2007], we conclude that definitive determination of the nature of the bloom will require further and more comprehensive in situ sampling to be carried out.

[42] **Acknowledgments.** We would like to thank the officers and crew of the RRS *Discovery*, the technical staff of the National Marine Facilities, and our fellow scientists for their hard work on the cruise. In particular, our thanks go to our colleague John Allen for getting the best out of SeaSoar on the cruise and processing much of the SeaSoar data. We are grateful to Alex Poulton and Mark Stinchcombe for providing biological and chemical data from the cruise. SeaWiFS data were obtained from NASA/GSFC, the Reynolds SST data from GHRSST, and sea surface height from AVISO. NEODAAS provided near real-time satellite data during the cruise. We are grateful for comments by reviewers on the paper that led to improvements in the revised version.

References

Blain, S., et al. (2007), Effect of natural iron fertilization on carbon sequestration in the Southern Ocean, *Nature*, *446*, 1070–1075.

Breitbarth, E., A. Oschilies, and J. LaRoche (2007), Physiological constraints on the global distribution of *Trichodesmium*—effect of temperature on diazotrophy, *Biogeosci.*, *4*, 53–61.

Calil, P. H. R., and K. J. Richards (2010), Transient upwelling hot spots in the oligotrophic North Pacific, *J. Geophys. Res.*, *115*, doi:10.1029/2009JC005360.

Capone, D. G., J. P. Zehr, H. W. Paerl, B. Bergman, and E. J. Carpenter (1997), *Trichodesmium*, a globally significant marine cyanobacterium, *Science*, *276*, 1221–1229.

da Silva, J. C. B., A. L. New, M. A. Srokosz, and T. J. Smyth (2002), On the observability of internal tidal waves in remotely-sensed ocean color data, *Geophys. Res. Lett.*, *29*, doi:10.1029/2001GL013888.

Davis, C. S., and D. J. McGillicuddy (2006), Transatlantic abundance of the N_2-fixing colonial cyanobacterium *Trichodesmium*, *Science*, *312*, 1517–1520.

de Ruijter, W. P. M., H. M. van Aken, J. R. E. Lutjeharms, R. P. Mantano, and M. W. Schouten (2004), Eddies and diploes around South Madagascar: Formation, pathways and large-scale impacts, *Deep-Sea Res. I*, *51*, 383–400.

DiMarco, S. F., P. Chapman, and W. D. Nowlin (2000), Satellite observations of upwelling on the continental shelf south of Madagascar, *Geophys. Res. Lett.*, *27*, 3965–3968.

Donohue, K. A., and J. M. Toole (2003), A near-synoptic survey of the Southwest Indian Ocean, *Deep Sea Res.*, *50*, 1893–1931.

Gregg, W. W. (2008), Assimilation of SeaWiFS ocean chlorophyll data into a three-dimensional global ocean model, *J. Mar. Sys.*, *69*, 205–225.

Huhn, F., A. von Kameke, V. Pérez-Muñuzuri, M. J. Olascoaga, and F. J. Beron-Vera (2012), The impact of advective transport by the South Indian Ocean countercurrent on the Madagascar bloom, *Geophys. Res. Lett.*, *39*, doi:10.1029/2012GL051246.

Koné, V., O. Aumont, M. Lévy, and L. Resplandy (2009), Physical and biogeochemical controls of the phytoplankton seasonal cycle in the Indian Ocean: A modeling study, pp. 147–166, in *Indian Ocean Biogeochemical Processes and Ecological Variability, Geophys. Mono. Ser*, vol. 185, AGU, Washington DC.

Lévy, M., D. Shankar, J.-M. André, S. S. C. Shenoi, F. Durand, and C. de Boyer Montégut (2007), Basin-wide seasonal evolution of the Indian Ocean's phytoplankton blooms, *J. Geophys. Res.*, *112*, C12014, doi:10.1029/2007JC004090.

Longhurst, A. (2001), A major seasonal phytoplankton bloom in the Madagascar Basin, *Deep-Sea Res. I*, *48*, 2413–2422.

Lutjeharms, J. R. E., and E. Machu (2000), An upwelling cell inshore of the East Madagascar Current, *Deep-Sea Res. I*, *47*, 2405–2411.

Machu, E., J. R. E. Lutjeharms, A. M. Webb, and H. van Aken (2002), First hydrographic evidence of the southeast Madagascar upwelling cell, *Geophys. Res. Lett.*, *29*, doi:10.1029/2002GL0015381.

Mahowald, N. M., et al. (2009), Atmospheric dust deposition: Global distribution, variability and human perturbations, *Ann. Rev. Mar. Sci. 1*, 245–278.

Marañón, E., et al. (2010), Degree of oligotrophy controls the response of microbial plankton to Saharan dust, *Limnol. Oceanogr.*, *55*, 2339–2352.

Mognin, M. M., E. R. Abraham, and T. W. Trull (2009), Winter advection of iron can explain the summer phytoplankton bloom that extends 1000 km downstream of the Kerguelen Plateau in the Southern Ocean, *J. Mar. Res.*, *67*, 225–237.

Monteiro, F. M., M. J. Follows, and S. Dutkiewicz (2010), Distribution of diverse nitrogen fixers in the global ocean, *Global Biogeochem. Cyc.*, *24*, doi:10.1029/2010GB003902.

Monteiro, F. M., M. J. Follows, and S. Dutkiewicz (2011), Biogeographical controls on the marine nitrogen fixers, *Global Biogeochem. Cyc.*, *25*, doi:10.1029/2009GB0037331.

Nassor, A., and M. R. Jury (1997), Intra-seasonal climate variability of Madagascar. Part 2: Evolution of flood events, *Meteorol. Atmos. Phys.*, *64*, 243–254.

Nassor, A., and M. R. Jury (1998), Intra-seasonal climate variability of Madagascar. Part 1: Mean summer conditions, *Meteorol. Atmos. Phys.*, *65*, 31–41.

Nauw, J. J., H M. van Aken, J. R. E. Lutjeharms, and W. P. M. de Ruijter, (2006), Intrathermocline eddies in the Southern Indian Ocean, *J. Geophys. Res.*, *111*, C03006, doi:10.1029/2005JC002917.

Nauw, J. J., H. M. van Aken, J. R. E. Lutjeharms, and W. P. M. de Ruijter (2008), Observations of the southern East Madagascar Current and undercurrent and countercurrent system, *J. Geophys. Res.*, *113*, C08006, doi:10.1029/2007JC004639.

Palastanga, V., P. J. van Leeuwen, M. W. Schouten, and W. P. M. de Ruijter (2007), Flow structure and variability in the subtropical Indian Ocean: Instability of the South Indian Counter Current, *J. Geophys. Res.*, *112*, C01001, doi:10.1029/2005JC003395.

Pidcock, R., M. Srokosz, J. Allen, M. Hartman, S. Painter, M. Mowlem, D. Hydes, and A. Martin (2010), A novel integration of an ultra-violet nitrate sensor on-board a towed vehicle for mapping open ocean submesoscale nitrate variability, *J. Atmos. Oceanic. Tech.*, *27*, 1410–1416.

Pollard, R., R. Sanders, M. Lucas, and P. Statham (2007), The Crozet natural iron bloom and export experiment, *Deep-Sea Res. II*, *54*, 1905–1914.

Pollard, R. T., et al. (2009), Southern ocean deep-water carbon export enhanced by natural iron fertilization, *Nature*, *457*, 577–581.

Poulton, A. J., M. C. Stinchcombe, and G. D. Quartly (2009), High numbers of *Trichodesmium* and diazotrophic diatoms in the southwest Indian Ocean, *Geophys. Res. Lett.*, *36*, L15610, doi:10.1029/2009GL0397179.

Quartly, G. D. (2006), Madagascar Experiment (MadEx), RRS Discovery Cruise 288, 26 Jan–21 Feb 2005, Cruise Report No. 8, National Oceanography Centre, Southampton, 105 pp. [Available at http://eprints.soton.ac.uk/42070/].

Quartly, G. D., J. J. H. Buck, M. A. Srokosz, and A. C. Coward (2006), Eddies around Madagascar—the retroflection re-considered, *J. Mar. Sys.*, *63*, 115–129.

Raj, R. P., B. N. Peter, and D. Pushadas (2010), Oceanic and atmospheric influences on the variability of phytoplankton bloom in the Southwestern Indian Ocean, *J. Mar. Sys.*, *82*, 217–229.

Reynolds, R. W., T. M. Smith, C. Liu, D. B. Chelton, K. S. Casey, and M. G. Schlax (2007), Daily high-resolution-blended analyses for sea surface temperature, *J. Clim.*, *20*, 5473–5492, doi:10.1175/2007JCLI1824.1.

Siedler, G., M. Rouault, A. Biastoch, E. Backeberg, C. J. C. Reason, and J. R. E. Lutjeharms (2009), Modes of the southern extension of the East Madagascar Current, *J. Geophys. Res.*, *114*, C01005, doi:10.1029/2008JC004921.

Smith R. C. (1981), Remote sensing and the depth distribution of ocean chlorophyll, *Mar. Ecol. Prog. Ser.*, *5*, 359–361.

Srokosz, M. A., A. P. Martin, and M. J. R. Fasham (2003), On the role of biological dynamics in plankton patchiness at the mesoscale: An example from the eastern North Atlantic Ocean, *J. Mar Res.*, *61*, 517–537.

Srokosz, M. A., G. D. Quartly, and J. J. H. Buck (2004), A possible plankton wave in the Indian Ocean, *Geophys. Res. Lett.*, *31*, L13301, doi:10.1029/2004GL109738.

Uz, B. M. (2007), What causes the sporadic phytoplankton bloom southeast of Madagascar? *J. Geophys. Res.*, *112*, C09010, doi:10.1029/2006JC003685.

Villareal, T. A., L. Adornato, C. Wilson, and C. A. Schoenbaechler (2011), Summer blooms of diatom-diazotroph assemblages and surface

chlorophyll in the North Pacific gyre: A disconnect, *J. Geophys. Res.*, *116*, C03001, doi:10.1029/2010JC006268.

Westberry T. K., and D. A. Siegel (2006), Spatial and temporal distribution of *Trichodesmium* blooms in the world's ocean, *Global Biogeochem. Cycles*, *20*, GB4016, doi:10.1029/2005GB002673.

Wilson, C. (2003), Late summer chlorophyll blooms in the oligotrophic North Pacific Subtropical Gyre, *Geophys. Res. Lett.*, *30*, 1942, doi:10.1029/2003GL017770.

Wilson, C., T. A. Villareal, N. Maximenko, S. J. Bograd, J. P. Montoya, and C. A. Schoenbaechler (2008), Biological and physical forcings of late summer chlorophyll blooms at 30°N in the oligotrophic Pacific, *J. Mar. Sys.*, *69*, 164–176.

Wilson, C., and X. Qiu (2008), Global distribution of summer chlorophyll blooms in the oligotrophic gyres, *Prog. Oceanogr.*, *78*, 107–134.

Yool, A., E. E. Popova, and T. R. Anderson (2011), MEDUSA-1.0: A new intermediate complexity plankton ecosystem model for the global domain, *Geosci. Model Dev.*, *4*, 381–417.